Computer simulation of charged hard spherocylinders

Carlos Avendaño, Alejandro Gil-Villegas, and Enrique González-Tovar

Citation: J. Chem. Phys. **128**, 044506 (2008); doi: 10.1063/1.2823736
View online: http://dx.doi.org/10.1063/1.2823736
View Table of Contents: http://jcp.aip.org/resource/1/JCPSA6/v128/i4
Published by the American Institute of Physics.

Computer simulation of charged hard spherocylinders

Carlos Avendaño
Facultad de Química, Universidad de Guanajuato, Noria Alta s/n, 36050 Guanajuato, Guanajuato, Mexico

Alejandro Gil-Villegas[a)]
Instituto de Física, Universidad de Guanajuato, Lomas del Bosque 103, 37150 León, Guanajuato, Mexico

Enrique González-Tovar
Instituto de Física, Universidad Autónoma de San Luis Potosí, Álvaro Obregón 64, 78000 San Luis Potosí, San Luis Potosí, Mexico

(Received 17 October 2007; accepted 20 November 2007; published online 28 January 2008)

In this work we present a computer simulation study of charged hard spherocylinders of aspect ratio $L/\sigma=5$, using *NVT* and *NPT* Monte Carlo methods. Coulombic interactions are handled using the Wolf method [D. Wolf, P. Keblinski, S. R. Phillpot, and J. Eggebrecht, J. Chem. Phys. **110**, 8254 (1999)]. Thermodynamic and structural properties are in excellent agreement with the results obtained with the standard Ewald summation method. A partial prediction of the corresponding phase diagram is obtained by studying two isotherms of this system. The stability of the liquid crystalline phases is examined and compared with the phase diagrams of neutral hard spherocylinders and dipolar hard spherocylinders. © *2008 American Institute of Physics*. [DOI: 10.1063/1.2823736]

I. INTRODUCTION

Dispersions of anisotropic colloids and several ionic liquids can show liquid crystalline phases.[1] Examples of these kinds of systems are rodlike colloidal particles and rodlike viruses that can exhibit orientational and positional order.[2] An accurate description of these complex materials is very important due to their broad applications in many advanced technologies and in connection with relevant theoretical issues such as ionic criticality. Over the years, theoretical work on charged elongated molecules has been published;[3–13] however, the analysis of these systems by molecular simulation is more demanding due to the high computational time needed to handle the long-range Coulomb potential using standard procedures such as the Ewald sum (ES) method.

A primitive model of charged rodlike particles consists on hard spherocylinders (HSCs) with point charges embedded in the body. A HSC is a cylinder of length L and diameter σ with hemispherical caps on each end; the geometry of these particles is completely characterized by the aspect ratio L/σ. It is well established since Onsager work[3] on colloidal liquid crystals a hard-core repulsive interaction is enough to induce the formation of a nematic (N) phase. Furthermore, molecular simulation studies have shown that a smectic-A (SmA) phase also exists for this system.[14,15]

The importance of the HSC representation resides in the fact that it can be used as a reference system for nonspherical models.[16] McGrother *et al.*[14] investigated the phase diagram of HSC using isothermal-isobaric (*NPT*) Monte Carlo simulations for several values of the aspect ratio. Two of the principal findings obtained in such study are that liquid crystalline (LC) phases can be observed only for values of L/σ around 3.2, and that the smectic-A phase is the first phase to be stable. Below this value of L/σ there are only two stable phases, an isotropic fluid (I) and a crystal. A HSC system with aspect ratio $L/\sigma=5$ presents isotropic, nematic, and smectic-A phases over a wide range of densities. Bolhuis and Frenkel have studied by molecular simulation the full phase diagram of HSC for aspect ratios from $L/\sigma=0$ to $L/\sigma=60$.[15]

Additional to short-ranged repulsive forces, other interactions are present in real mesogens, and it is important o determine their effects in the formation of LC states. In particular, the behavior of HSC plus dipolar interactions (DHSC) has been studied by several authors.[17–25] We can summarize the main conclusions from these articles as follows. When the dipole is located at the center of the molecule, either parallel or transverse to the molecular axis, the nematic phase becomes unstable compared with the nonpolar case as the temperature decreases and an I-N-SmA triple point appears. If the dipole is located at the end of the molecule with a longitudinal orientation, a mild destabilization of the nematic phase with respect to the isotropic state was detected, when compared again with respect to the neutral case, and the smectic phase is destabilized relative to the nematic phase. No evidence of ferroelectric or antiferroelectric behavior was found. In the case of DHSC with central transverse point dipoles, an interesting effect appears when smectic phases are formed, since the dipoles are contained within the smectic layers. At high temperatures the dipolar configurations are random, without any preferred orientation. However, as the temperature decreases, chain and ring dipolar patterns are formed, suggesting that two different types of smectic phases are present in this system depending on the arrangement of the dipoles within the smectic layers.[22]

A system of charged hard spherocylinders (CHSC) is interesting not only for its use as a primitive model of real

[a)]Electronic mails: gil@fisica.ugto.mx and agilvm@gmail.com.

TABLE I. Monte Carlo computer simulation results for the excess internal energy U^{exc}/NkT and order parameter S for a system $N=1020$ charged hard spherocylinders with aspect ratio $L/\sigma=5$. Results obtained using the Ewald sum and Wolf methods in a NVT ensemble. Liquid crystalline phases nomenclature is I=Isotropic, N=Nematic, and SmA=Smectic A.

$\bar{T}^*$	η	Phase	$-U^{exc}/NkT$	S	Method
1.0	0.35	I	0.262 ± 0.008	0.050 ± 0.018	Wolf
1.0	0.35	I	0.269 ± 0.008	0.051 ± 0.016	Ewald
1.0	0.45	N	0.304 ± 0.009	0.760 ± 0.011	Wolf
1.0	0.45	N	0.311 ± 0.008	0.752 ± 0.013	Ewald
1.0	0.55	SmA	0.411 ± 0.007	0.965 ± 0.004	Wolf
1.0	0.55	SmA	0.412 ± 0.010	0.945 ± 0.007	Ewald
0.5	0.35	I	0.634 ± 0.013	0.053 ± 0.019	Wolf
0.5	0.35	I	0.645 ± 0.013	0.051 ± 0.019	Ewald
0.5	0.45	N	0.738 ± 0.015	0.757 ± 0.015	Wolf
0.5	0.45	N	0.742 ± 0.013	0.757 ± 0.018	Ewald
0.5	0.55	SmA	0.942 ± 0.013	0.954 ± 0.004	Wolf
0.5	0.55	SmA	0.931 ± 0.012	0.969 ± 0.002	Ewald

substances where the interplay of charge and shape of the molecule determines novel phases but also because it is a generalization of simpler idealizations of an electrolyte, such as the primitive model of spherical electrolytes, which over the years has originated a vivid debate in reference to its critical behavior. Notice that by choosing $L/\sigma=0$, the CHSC system reduces to the well-known restricted primitive model (RPM) of electrolytes, a model that has played a fundamental role in our understanding of ionic systems.

In order to study the phase diagram of charged hard spherocylinders, we need to deal with the long-range nature of the Coulombic interaction. Standard methods to handle electrostatic interactions in computer simulation are the Ewald sum[26–28] and the Onsager reaction-field methods.[29] Alternatively, Wolf and co-workers[30,31] proposed to simulate systems with electrostatic interactions through the use of an electroneutral spherical cavity surrounding a certain number of particles. The Wolf method can be implemented using standard periodic boundary conditions and the minimum-image convention, and then a considerable reduction in computational time is obtained in comparison with the standard Ewald sum method. Demontis *et al.*[32] applied the Wolf procedure in molecular dynamics (MD) of aluminosilicates and liquid water, while Zahn *et al.*[33] modified the Wolf method to compute by MD the properties of water. Ma and Garofalini[34] used the Wolf procedure, which was corrected to include the effect of the charge overlap, to model covalent systems such as SiC and SiO_2. Avendaño and Gil-Villegas studied primitive models of electrolytes using Monte Carlo simulation with the Wolf method,[35] finding that the Wolf scheme can be implemented for a great variety of systems with high asymmetries in size and charge using only one set of values for the two parameters that are involved in the Wolf binary potential for electrostatic systems. The Wolf method was found to give also very accurate results for hard spheres with extended dipoles produced by point charges.[36] For the case of hard spheres with point dipoles, a truncated version of the Ewald sum that basically follows the scheme of the Wolf method[37] also predicts very well the properties of this system. Fennell and Gezelter[38] contrasted favorably thermodynamic and dynamic properties of different systems obtained from the standard and Zanh versions of the Wolf method. Mahadevan and Garofalini[39] and, recently, Carré *et al.*[40] studied water with a dissociative potential and liquid silica, respectively, using molecular dynamics with the Wolf method.

In this paper, we address the problem of applying the Wolf method to study nonspherical particles and liquid-crystalline phases using the CHSC system of aspect ratio $L/\sigma=5$. The contents of this article are as follows. In Sec. II, we summarize the Wolf method. In Sec. III, we discuss the computer simulation details, whereas in Sec. IV we report the results of thermodynamic, structure, and two isotherms of the phase diagram of CHSC. Finally, in Sec. V we give our conclusions.

II. THE WOLF METHOD

As a consequence of the long-range behavior of the Coulombic potential, computer simulations of charged systems cannot be performed with the standard periodic-boundary conditions and the minimum-image convention, but special methods are needed, such as the ES method. In the ES, the conditionally convergent energy sum over all pair of charges is split into three totally convergent terms: a term evaluated in real space, another one calculated in the reciprocal space, and a third one that accounts for a self-interaction contribution. The shortcoming of the ES method is that the reciprocal space term can be highly expensive in time. Since a proper stabilization in a Monte Carlo (MC) run for charged systems usually needs a large number of cycles, efficient ways of implementing the ES method are required.

The Wolf procedure[30,31] is an alternative route to evaluate electrostatic interactions in a faster way than the Ewald summation, based on a truncation of the Coulombic potential at a given distance, R_C. By correcting the potential produced by the charges inside the cavity, in order to guarantee that the net charge within the cavity is null, the energy will fluctuate

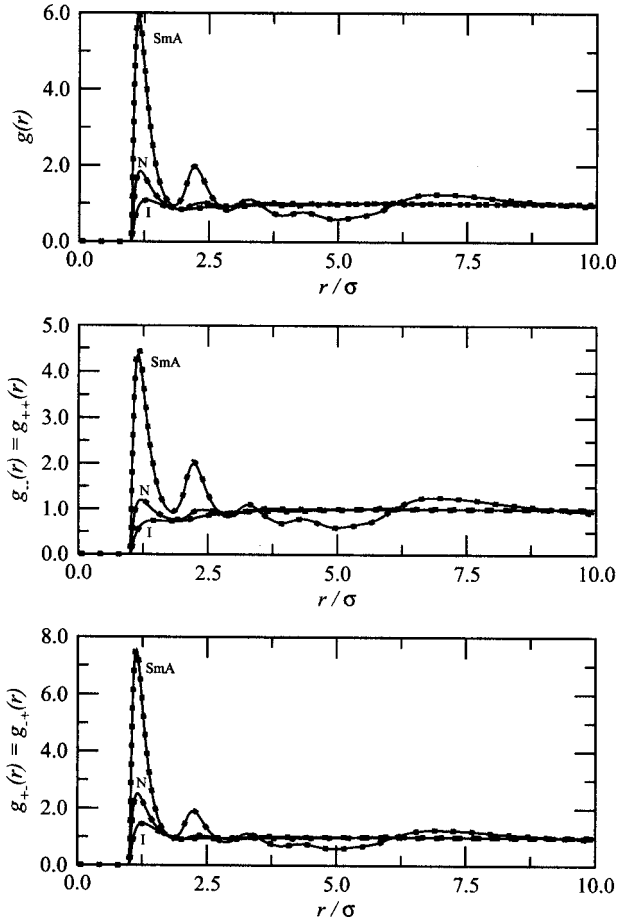

FIG. 1. The distribution functions $g(r)$, $g_{++}(r)$, and $g_{+-}(r)$ for 1020 charged hard spherocylinders of aspect ratio $L/\sigma=5$ at a temperature of $T^*=1.0$, obtained by Monte Carlo computer simulations in the *NVT* ensemble. Solid lines and symbols correspond to Ewald sum and Wolf methods results, respectively.

around the correct thermodynamic limit value. Accordingly, the total electrostatic energy in the Wolf procedure is then given by

$$U(R_C) = \frac{1}{2}\sum_{i=1}^{N} \sum_{\substack{j\neq i \\ (r_{ij}<R_C)}} \left(\frac{q_i q_j \,\mathrm{erfc}(\alpha r_{ij})}{r_{ij}} - \frac{q_i q_j \,\mathrm{erfc}(\alpha R_c)}{R_C} \right) - \left(\frac{\mathrm{erfc}(\alpha R_c)}{2R_C} + \frac{\alpha}{\pi^{1/2}} \right) \sum_{i=1}^{N} q_i^2, \quad (1)$$

where the first term in the right-hand side of Eq. (1) is the effective potential between a pair of particles and the second term is a self-constant term. This equation depends on two parameters that need to be optimized, namely, R_C and the damping parameter α that determines the range of the effective potential. As it has been discussed in previous work, it is possible to describe a wide variety of electrolyte systems using the same set of values for α and R_C.[35]

III. SIMULATION DETAILS

The behavior of 1:1 CHSC with point charges fixed at the center of the body was studied using Monte Carlo simulation in the *NVT* and *NPT* ensembles.[41,42] The interaction between a pair of particles is given by

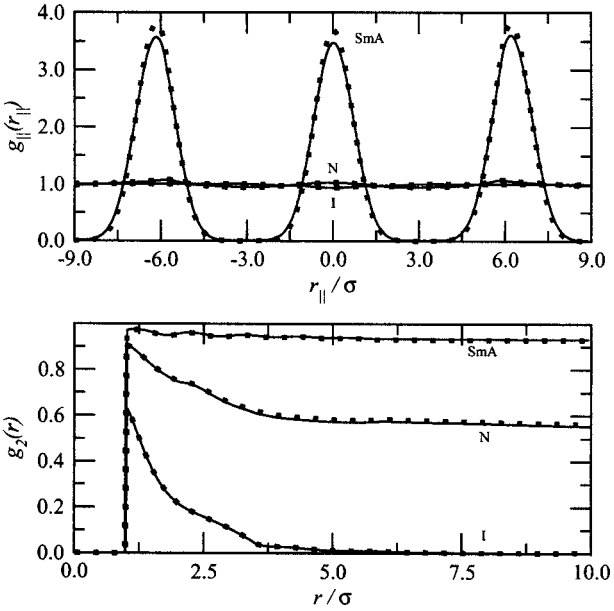

FIG. 2. The distribution functions $g_{\|}(r_{\|})$ and $g_2(r)$ for 1020 charged hard spherocylinders of aspect ratio $L/\sigma=5$ at a temperature of $T^*=1.0$, obtained by Monte Carlo computer simulations in the *NVT* ensemble. Solid lines and symbols correspond to Ewald sum and Wolf methods results, respectively.

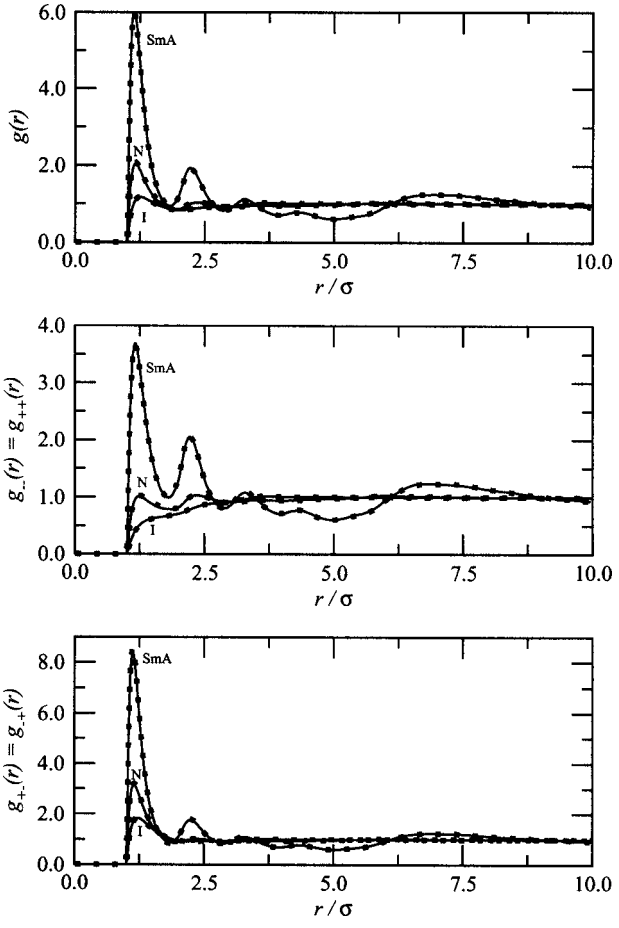

FIG. 3. The distribution functions $g(r)$, $g_{++}(r)$, and $g_{+-}(r)$ for 1020 charged hard spherocylinders of aspect ratio $L/\sigma=5$ at a temperature of $T^*=0.5$, obtained by Monte Carlo computer simulations in the *NVT* ensemble. Solid lines and symbols correspond to Ewald sum and Wolf methods results, respectively.

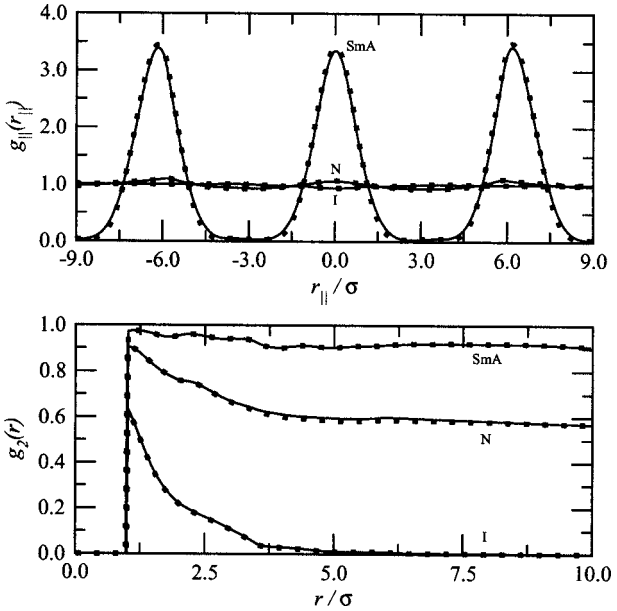

FIG. 4. The distribution functions $g_{\parallel}(r_{\parallel})$ and $g_2(r)$ for 1020 charged hard spherocylinders of aspect ratio $L/\sigma=5$ at a temperature of $T^*=0.5$, obtained by Monte Carlo computer simulations in the *NVT* ensemble. Solid lines and symbols correspond to Ewald sum and Wolf methods results, respectively.

$$u_{ij} = u_{ij}^{\mathrm{hb}}(\mathbf{r}_{ij}, \omega_i, \omega_j) + \frac{q_i q_j}{D r_{ij}}, \tag{2}$$

where q_i is the charge of the particle i, D is the dielectric constant of the surrounding media, $\mathbf{r}_{ij}$ is the interparticle vector between the centers of mass of the entities i and j, $r_{ij} = |\mathbf{r}_{ij}|$, and u^{hb} is the hard body interaction, i.e.,

$$u_{ij}^{\mathrm{hb}}(\mathbf{r_{ij}}, \omega_i, \omega_j) = \begin{cases} \infty & \text{if } \mathbf{r_{ij}} \in V_{\mathrm{ex}}(\omega_i, \omega_j) \\ 0 & \text{if } \mathbf{r_{ij}} \notin V_{\mathrm{ex}}(\omega_i, \omega_j), \end{cases} \tag{3}$$

where ω_i denotes the orientation of the molecular axis of the particle i and V_{ex} is the volume excluded by ions i and j. Reduced variables are introduced: temperature, pressure, and packing fraction, defined as $T^*=kTD\sigma/(z_+z_-e^2)$, $P^*=Pv_{\mathrm{HSC}}/(kT)$, and $\eta=Nv_{\mathrm{HSC}}/V$, wherein k is the Boltzmann constant, T is the absolute temperature, σ is the diameter of the particles, z_i is the valence of the species i, e is the protonic charge, N is the total number of particles, V is the volume, P is the pressure, and v_{HSC} is the volume of a hard spherocylinder molecule, given by $v_{\mathrm{HSC}}=(\pi\sigma^3/6)+(\pi\sigma^2L/4)$.

A face centered cubic (fcc) lattice was used as the initial configuration.[14,43] This structure was built using a fcc array of hard spheres with the [111] direction along the z axis, and then the distance between the close-packed [111] planes was scaled by the length of the spherocylinder. The unit cell in the fcc lattice has six particles. By the replication of this cell in three perpendicular directions, a near-cubic simulation box can be obtained using specific values of the replication factors, which must be determined according to the number of particles, as detailed in Table I in Ref. 14. For the *NVT* simulations, the initial fcc lattice was expanded to the desired density and equilibrated at such state. For the *NPT* simulations, the fcc array was also expanded into a low-density isotropic state and equilibrated, and then the reduced pressure was gradually increased in order to obtain higher-density thermodynamic states within an isotherm.

Computer simulations were performed using the Wolf and ES methods, in order to determine the best values for the

TABLE II. Isothermal-isobaric Monte Carlo results for the pressure P^*, packing fraction η, order parameter S, excess internal energy U^{exc}/NKT, and type of liquid crystalline phase. Results obtained using the Wolf method for a system of $N=1020$ charged hard spherocylinders with $L/\sigma=5$ at a temperature of $T^*=1.0$. Liquid crystalline phase nomenclature is I=Isotropic, N=Nematic, and SmA=Smectic A.

P^*	η	S	$-U^{\mathrm{exc}}/NkT$	Phase
1.00	0.215 ± 0.002	0.031 ± 0.011	0.212 ± 0.009	*I*
2.00	0.284 ± 0.002	0.037 ± 0.013	0.237 ± 0.008	*I*
3.00	0.330 ± 0.002	0.036 ± 0.014	0.256 ± 0.009	*I*
4.00	0.367 ± 0.002	0.050 ± 0.019	0.267 ± 0.009	*I*
4.25	0.376 ± 0.002	0.099 ± 0.037	0.270 ± 0.010	*I*
4.50	0.384 ± 0.002	0.083 ± 0.027	0.277 ± 0.009	*I*
4.75	0.393 ± 0.002	0.083 ± 0.034	0.283 ± 0.009	*I*
5.00	0.400 ± 0.002	0.146 ± 0.040	0.286 ± 0.012	*I*
5.25	0.410 ± 0.003	0.169 ± 0.025	0.289 ± 0.010	*I*
5.50	0.418 ± 0.002	0.213 ± 0.052	0.294 ± 0.009	*I*
5.75	0.427 ± 0.002	0.243 ± 0.047	0.296 ± 0.008	*I*
6.00	0.444 ± 0.003	0.740 ± 0.023	0.304 ± 0.009	*N*
6.25	0.453 ± 0.003	0.786 ± 0.016	0.306 ± 0.009	*N*
6.50	0.463 ± 0.003	0.823 ± 0.015	0.316 ± 0.008	*N*
6.75	0.490 ± 0.003	0.887 ± 0.009	0.353 ± 0.010	SmA
7.00	0.506 ± 0.003	0.927 ± 0.006	0.370 ± 0.007	SmA
7.25	0.512 ± 0.003	0.924 ± 0.006	0.377 ± 0.011	SmA
7.50	0.520 ± 0.003	0.936 ± 0.006	0.383 ± 0.009	SmA
7.75	0.527 ± 0.003	0.942 ± 0.006	0.383 ± 0.009	SmA
8.00	0.534 ± 0.003	0.945 ± 0.005	0.396 ± 0.012	SmA
8.20	0.540 ± 0.002	0.948 ± 0.006	0.397 ± 0.010	SmA

TABLE III. Isothermal-isobaric Monte Carlo results for the pressure P^*, packing fraction η, order parameter S, excess internal energy U^{exc}/NkT, and type of liquid crystalline phase. Results obtained using the Wolf method for a system of $N=1020$ charged hard spherocylinders with $L/\sigma=5$ at a temperature of $T^*=0.5$. Liquid crystalline phase nomenclature is I=Isotropic, N=Nematic, and SmA=Smectic A.

P^*	η	S	$-U^{exc}/NkT$	Phase
1.00	0.218 ± 0.002	0.031 ± 0.011	0.522 ± 0.012	I
2.00	0.286 ± 0.002	0.037 ± 0.013	0.578 ± 0.012	I
3.00	0.332 ± 0.002	0.046 ± 0.019	0.617 ± 0.013	I
4.00	0.369 ± 0.002	0.060 ± 0.017	0.654 ± 0.013	I
4.25	0.378 ± 0.002	0.082 ± 0.026	0.660 ± 0.014	I
4.50	0.386 ± 0.002	0.092 ± 0.026	0.668 ± 0.012	I
4.75	0.394 ± 0.002	0.166 ± 0.026	0.675 ± 0.014	I
5.00	0.404 ± 0.002	0.116 ± 0.022	0.687 ± 0.011	I
5.25	0.412 ± 0.002	0.207 ± 0.027	0.694 ± 0.015	I
5.50	0.425 ± 0.003	0.474 ± 0.033	0.710 ± 0.012	N
5.75	0.441 ± 0.002	0.723 ± 0.024	0.721 ± 0.013	N
6.00	0.452 ± 0.002	0.795 ± 0.011	0.737 ± 0.014	N
6.25	0.467 ± 0.003	0.844 ± 0.014	0.779 ± 0.015	N
6.50	0.494 ± 0.002	0.905 ± 0.006	0.859 ± 0.012	SmA
6.75	0.503 ± 0.002	0.908 ± 0.007	0.873 ± 0.013	SmA
7.00	0.512 ± 0.002	0.924 ± 0.007	0.890 ± 0.013	SmA
7.25	0.518 ± 0.002	0.921 ± 0.007	0.894 ± 0.014	SmA
7.50	0.523 ± 0.002	0.927 ± 0.005	0.894 ± 0.015	SmA
7.75	0.529 ± 0.002	0.928 ± 0.006	0.894 ± 0.015	SmA
8.00	0.537 ± 0.002	0.933 ± 0.005	0.914 ± 0.013	SmA
8.25	0.542 ± 0.002	0.936 ± 0.005	0.922 ± 0.015	SmA

parameters of the Wolf potential. We found that the same set of values used in our previous account of primitive models of electrolytes[35] can reproduce the ES results for the same LC systems considered here. The values of the parameters used were $\alpha=4.0/\mathcal{L}_{\min}$ and $R_C=0.5\mathcal{L}_{\min}$ for the case of the Wolf method, and $\alpha=5.0/\mathcal{L}_{\min}$ and 518 $\mathbf{k}$ vectors for the ES (that corresponds to $n_{\max}=6$), where $\mathcal{L}_{\min}$ is the shortest simulation box length. An *NVT* cycle consists of N trial displacements and reorientations of the particles. In most of our simulations, $1\times10^6-2\times10^6$ cycles were required to equilibrate the systems in the *NVT* simulations and the same number of cycles was completed to obtain average values. Only in those states near the phase transitions and at high densities more cycles were required. The changes on positions and orientations were adjusted to achieve a 30%–45% acceptance probability. In the *NPT* ensemble every *NVT* cycle was supplemented with a change on the system volume.

The formation of ordered phases was established using the nonvanishing values of the nematic order parameter defined as

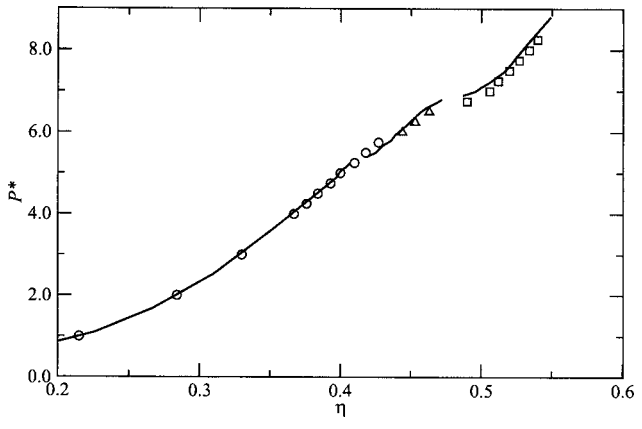

FIG. 5. The pressure P^* as a function of the packing fraction η for a system of 1020 charged hard spherocylinders of aspect ratio $L/\sigma=5$ at a temperature of $T^*=1.0$, obtained by Monte Carlo computer simulations and the Wolf method in the *NPT* ensemble. Circles, triangles, and squares correspond to the CHSC isotropic, nematic, and smectic-A branches, respectively. The solid line represents the data for a system of 1020 hard spherocylinders (Ref. 14).

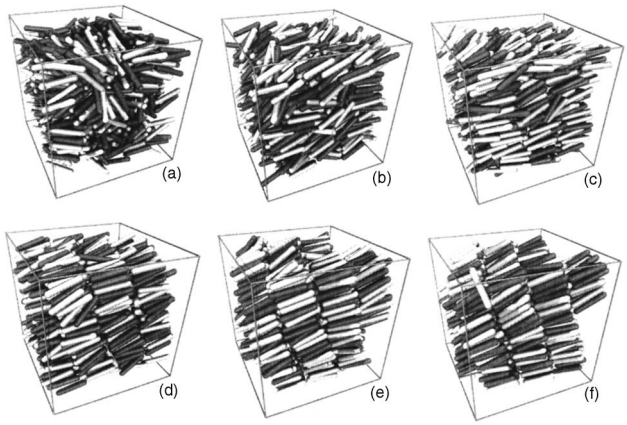

FIG. 6. Snapshots for different configurations for 1020 charged hard spherocylinders of aspect ratio $L/\sigma=5$ at a temperature of $T^*=1.0$, obtained by Monte Carlo computer simulations and the Wolf method in the *NPT* ensemble. The configurations correspond to (a) the highest-density isotropic state ($P^*=5.75$), (b) the lowest-density nematic state ($P^*=6.00$), (c) the highest-density nematic state ($P^*=6.50$), (d) the lowest-density smectic-A state ($P^*=6.75$), (e) a middle-density smectic-A state ($P^*=7.50$), and (f) the highest-density smectic-A state ($P^*=8.25$).

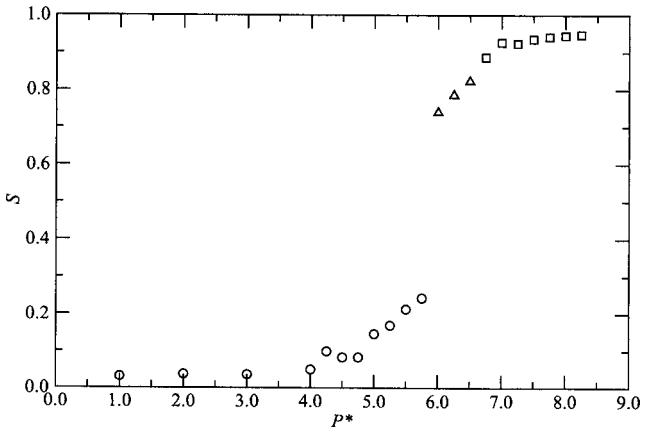

FIG. 7. The nematic order parameter S as a function of the pressure P^* for a system of 1020 charged hard spherocylinders of aspect ratio $L/\sigma=5$ at a temperature of $T^*=1.0$, obtained by Monte Carlo computer simulations and the Wolf method in the *NPT* ensemble. Circles, triangles, and squares correspond to the CHSC isotropic, nematic, and smectic-A branches, respectively.

$$S = \frac{1}{N}\sum_{i=1}^{N} P_2(\cos\theta_i), \tag{4}$$

where $P_2(\cos\theta_i)$ is the second Legendre polynomial and θ_i is the angle between the director $\mathbf{n}$ and the principal molecular axis of the particle i. The preference direction given by the director $\mathbf{n}$ is not known *a priori* and then the order parameter needs to be evaluated using the ordering matrix tensor $\mathbf{Q}$:

$$\mathbf{Q} = \frac{1}{N}\sum_{i=1}^{N}\left(\frac{3}{2}\mathbf{u}_i\mathbf{u}_i - \frac{\mathbf{I}}{2}\right), \tag{5}$$

where $\mathbf{u}_i$ is a unit vector along the principal axis of the molecule i and $\mathbf{I}$ is the unit tensor. When $\mathbf{Q}$ is diagonalized, the order parameter is obtained from the largest eigenvalue, with the director as the corresponding eigenvector. To complete the characterization of the system, several distribution functions were also calculated: the radial distribution function $(g(r))$, the charge-charge radial distribution functions $(g(r)_{--}, g(r)_{++}, g(r)_{+-})$, the orientational correlation function

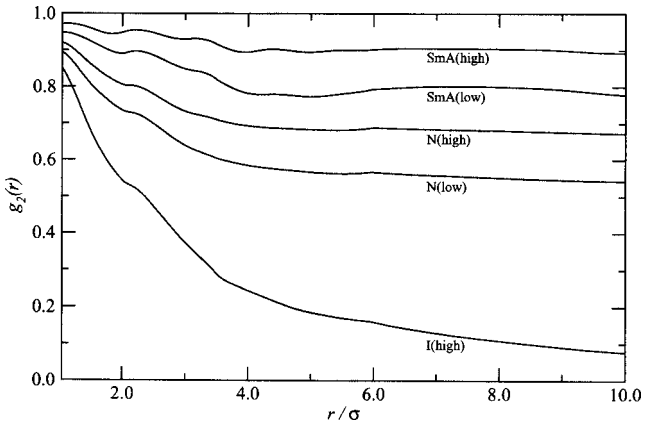

FIG. 8. The orientational pair correlation function $g_2(r)$ for a system of 1020 charged hard spherocylinders of aspect ratio $L/\sigma=5$ at a temperature of $T^*=1.0$, obtained by Monte Carlo computer simulations and the Wolf method in the *NPT* ensemble. The lines correspond to the results for the same states shown in Fig. 6.

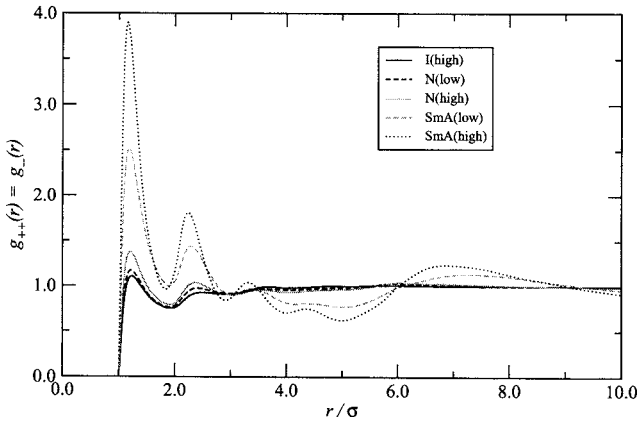

FIG. 9. The pair radial distribution function $g_{++}(r)$ for a system of 1020 charged hard spherocylinders of aspect ratio $L/\sigma=5$ at a temperature of $T^*=1.0$, obtained by Monte Carlo computer simulations and the Wolf method in the *NPT* ensemble. The lines correspond to (a) the highest-density isotropic state ($P^*=5.75$), (b) the lowest-density nematic state ($P^*=6.00$), (c) the highest-density nematic state ($P^*=6.50$), (d) the lowest-density smectic-A state ($P^*=6.75$), and (e) the highest-density smectic-A state ($P^*=8.25$).

$(g_2(r)$, calculated as the average value of the second order Legendre's polynomial for the angle between a pair of particles), and the distribution function for the projection of the relative position between particles along the director, $(g_\parallel(r_\parallel))$, which is used to detect the appearance of smectic phases.

IV. RESULTS

A. Comparison between the Wolf and Ewald sum methods

As a first goal, we examined the equivalence between the Ewald and Wolf methods, for a system of CHSC. Structural as well as thermodynamic properties were simulated applying both schemes. Using a *NVT*-MC method, six different states were surveyed for a system of 1020 charged hard spherocylinders. Three packing fractions were considered, $\eta=0.35, 0.45, 0.55$, for two different temperatures, $T^*=1.0, 0.5$. We report in Table I the corresponding simulation results for the excess internal energy U^{exc}/NkT and the order parameter S. The values of the parameters required in both methods have been given in the previous section; in the case of the Wolf method, these parameters have the same values as the ones used in a prior article about simple electrolytes.[35] From this table it is clear that both methods are equivalent since the predicted energies and order parameters are within the uncertainty of the simulations. A further analysis of this equivalence was done by simulating different distribution functions at the same thermodynamic states used before. In Figs. 1 and 2 the distribution functions $g(r)$, $g_{++}(r)$, $g_{+-}(r)$, $g_\parallel(r_\parallel)$, and $g_2(r)$ are portrayed for the temperature $T^*=1.0$ and in Figs. 3 and 4 the same functions are displayed for the temperature $T^*=0.5$. For all the cases, a very accurate agreement was found between the ES and Wolf predictions, and the same LC phases are reproduced. A small systematic deviation can be observed for the $g_\parallel(r_\parallel)$ function, where for the smectic phases the Wolf method predicts better defined peaks than in the case of the corresponding Ewald data, although the discrepancy between the results is very small. A similar

TABLE IV. Comparative table of properties (pressure, packing fraction and order parameter) in states nearby a phase transition, for three different models: HSC (Refs. 14), dipolar HSC (DHSC) with central longitudinal dipoles (Ref. 23), and charged HSC (CHSC) (this work).

		I–N transition			N-SmA transition		
Models	T^*	$P^*_{I\text{–}N}$	$\eta_I-\eta_N$	S_I-S_N	$P^*_{N\text{–SmA}}$	$\eta_N-\eta_{\text{SmA}}$	S_N-S_{SmA}
HSC	⋯	5.31	0.407–0.415	0.215–0.471	6.85	0.472–0.487	0.857–0.893
DHSC	1.0	6.06	0.432–0.438	0.185–0.398	6.56	0.460–0.476	0.785–0.872
CHSC	1.0	5.88	0.427–0.444	0.293–0.740	6.63	0.463–0.490	0.823–0.887
CHSC	0.5	5.38	0.412–0.425	0.207–0.474	6.30	0.467–0.494	0.844–0.905

feature was reported previously[21] for dipolar HSC when the Onsager reaction-field and Ewald methods were compared. In the CHSC system these differences are only significant at the position of the peaks, whereas for other positions there is not a noticeable deviation between the ES and Wolf methods.

Due to the very good agreement obtained between the ES and Wolf procedures, the phase diagram for the CHSC was studied using solely the Wolf method, which is faster than the ES, not only because in the first method it is unnecessary to evaluate a Fourier-like term but also because the volume subroutine in a *NPT* simulation can be efficiently implemented with the Wolf method through a simple scaling procedure, similar to the one used for the reaction field method,[23] which cannot be performed with the ES technique.

B. Isotherms of the phase diagram of charged hard spherocylinders

Monte Carlo simulations in the isobaric-isothermal (*NPT*) ensemble were performed to study isotherms of the phase diagram of CHSC. Two isotherms were determined, $T^*=1.0$ and $T^*=0.5$. Values of the packing fraction (η), pressure (P^*), excess internal energy (U^{exc}/NkT), order parameter (S), and type of phase are given in Tables II and III, respectively. The behavior of the pressure as a function of the packing fraction for this system at $T^*=1.0$ is shown in Fig. 5. The *I*-*N* transition can be determined from the direct visualization of equilibrium configurations (Fig. 6), from the search of discontinuities in the order parameter (Fig. 7), and also from the behavior of correlation functions as $g_2(r)$ (Fig. 8). At this temperature, an *I*-*N* transition from an isotropic state ($\eta\sim0.427$, $S\sim0.243$) to a nematic state ($\eta\sim0.444$, $S\sim0.740$) is observed at $P^*\sim5.875$. In Fig. 5, it can be noted that the nematic phase is destabilized with respect to the isotropic phase, similar to the case of hard spherocylinders with longitudinal central dipoles (DHSC) at the same temperature, although the transition pressure is slightly lower for CHSC (see Table IV). This effect in a DHSC fluid is consequence of pairing between particles, as pointed out in Refs. 23 and 44.

With respect to the density range of the nematic phase, CHSC and DHSC are coincident. The values of the order parameter become very high in the isotropic state due to the coupling at short distances between ions of different charge signs, as can be seen from the analysis of the charge-charge radial distribution functions in Figs. 9 and 10. The formation of layers in the smectic-A phase was detected from $g_{\parallel}(r_{\parallel})$, which is the distribution function of the projection along the director of the relative positions between particles (see Fig. 11). The *N*-SmA transition from a nematic state ($\eta\sim0.463$, $S\sim0.823$) to a smectic-A state ($\eta\sim0.490$, $S\sim0.887$) occurs at $P^*\sim6.625$.

In comparison with the phase diagram of hard spherocylinders, the CHSC nematic branch is destabilized with respect to the isotropic phase. The pair correlation function that describes the degree of orientational order, $g_2(r)$, is presented in Fig. 8 for different phases.

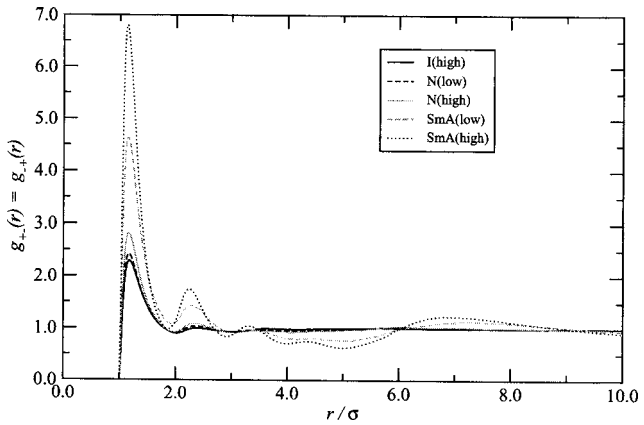

FIG. 10. The pair radial distribution function $g_{+-}(r)$ for a system of 1020 charged hard spherocylinders of aspect ratio $L/\sigma=5$ at a temperature of $T^*=1.0$, obtained by Monte Carlo computer simulations and the Wolf method in the *NPT* ensemble. The lines correspond to the results for the same states shown in Fig. 6.

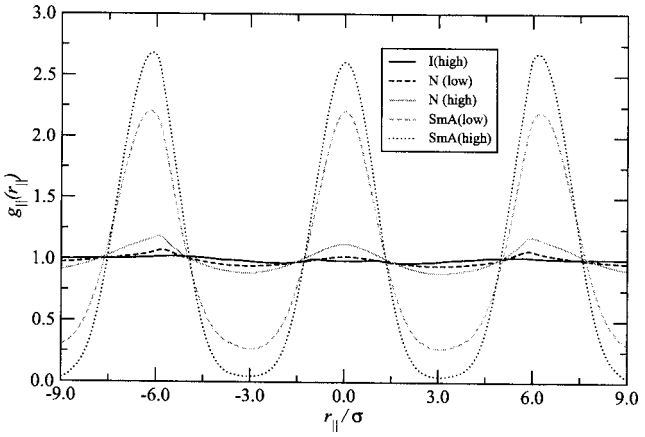

FIG. 11. The distribution function $g_{\parallel}(r_{\parallel})$ for a system of 1020 charged hard spherocylinders of aspect ratio $L/\sigma=5$ at a temperature of $T^*=1.0$, obtained by Monte Carlo computer simulations and the Wolf method in the *NPT* ensemble. The lines correspond to the results for the same states shown in Fig. 6.

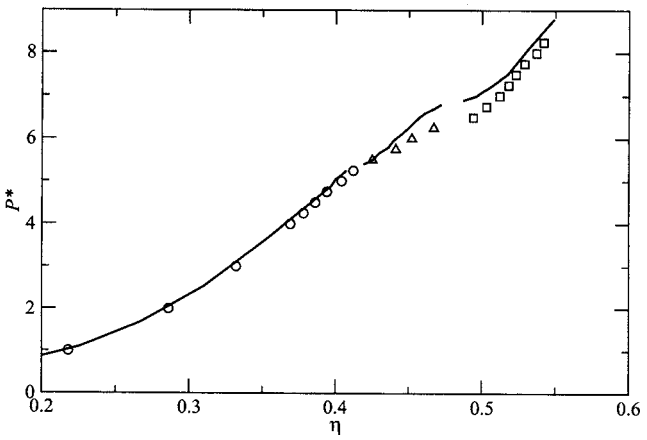

FIG. 12. The pressure P^* as a function of the packing fraction η for a system of 1020 charged hard spherocylinders of aspect ratio $L/\sigma=5$ at a temperature of $T^*=0.5$, obtained by Monte Carlo computer simulations and the Wolf method in the *NPT* ensemble. Circles, triangles, and squares correspond to the CHSC isotropic, nematic, and smectic-A branches, respectively. The solid line represents the data for a system of 1020 hard spherocylinders (Ref. 14).

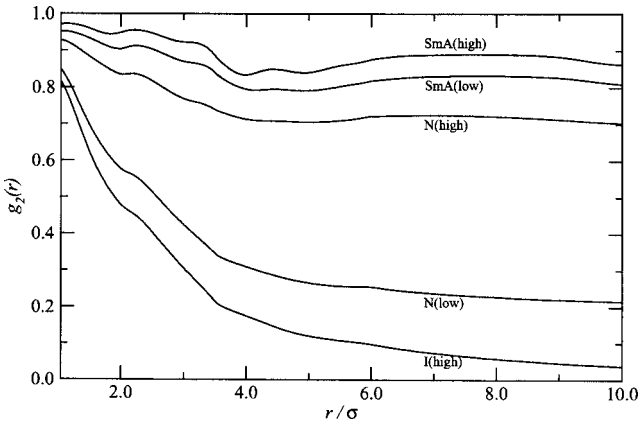

FIG. 14. The orientational pair correlation function $g_2(r)$ for a system of 1020 charged hard spherocylinders of aspect ratio $L/\sigma=5$ at a temperature of $T^*=0.5$, obtained by Monte Carlo computer simulations and the Wolf method in the *NPT* ensemble. The lines correspond to the highest-density isotropic state ($P^*=5.25$), the lowest-density nematic state ($P^*=5.50$), the highest-density nematic state ($P^*=6.25$), the lowest-density smectic-A state ($P^*=6.50$), and the highest-density smectic-A state ($P^*=8.25$).

The isotherm corresponding to the temperature $T^*=0.5$ is reported in Fig. 12. The depicted *I-N* transition is from an isotropic state ($\eta\sim0.412$, $S\sim0.207$) to a nematic state ($\eta\sim0.425$, $S\sim0.474$) at $P^*\sim5.38$. At this temperature the stabilization of the nematic phase with respect to the isotropic and Sm-A phases is similar to the case of HSC. Other properties and distributions functions are detailed in Figs. 13–17. From Figs. 12 and 13, we observe that the *N*-SmA transition occurs at $P^*\sim6.373$ between a nematic state ($\eta\sim0.467$, $S\sim0.844$) and a smectic-A state ($\eta\sim0.494$, $S\sim0.905$). Corresponding snapshots of distinct configurations are depicted in Fig. 18. As in the case for $T^*=1.0$, the interlayer defects in the smectic-A phases vanish at higher densities.

V. CONCLUSIONS

In this work, we have studied the behavior of charged hard spherocylinders with an aspect ratio of $L/\sigma=5$ using Monte Carlo simulations and the Wolf method. We have shown that the equivalence between Ewald and Wolf methods to predict the liquid-crystalline phases formed by CHSC can be obtained using the same set of values for the parameters R_C and α that were previously used to survey symmetric and asymmetric spherical electrolytes.[35] Computer simulations of charged systems using the Wolf method can be implemented easily in the form of a system of particles interacting via a binary short-ranged potential, in combination with standard procedures such as periodic-boundary conditions and minimum-image convention.

Two isotherms of the phase diagram of CHSC have been analyzed by means of *NPT* MC simulations. For the temperature $T^*=1.0$ the CHSC system has similar phase properties as those of the DHSC system with central point longitudinal dipoles. However, at the temperature $T^*=0.5$, the ranges of η for the CHSC phases are closer to the corresponding ranges of the nonpolar HSC system. A more detailed analysis of the phase diagram of the CHSC system,

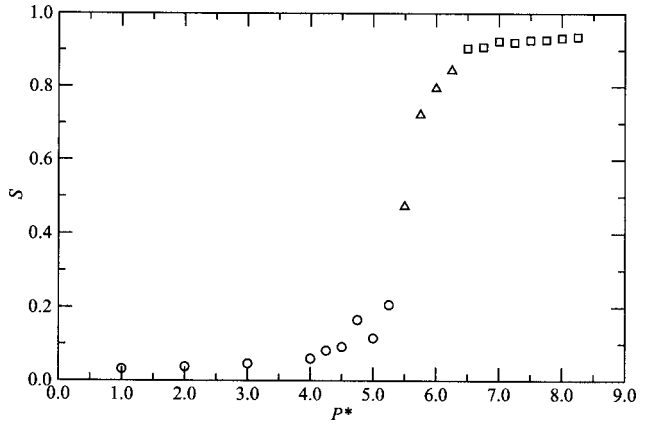

FIG. 13. The nematic order parameter S as a function of the pressure P^* for a system of 1020 charged hard spherocylinders of aspect ratio $L/\sigma=5$ at a temperature of $T^*=0.5$, obtained by Monte Carlo computer simulations and the Wolf method in the *NPT* ensemble. Circles, triangles, and squares correspond to the CHSC isotropic, nematic, and smectic-A branches, respectively.

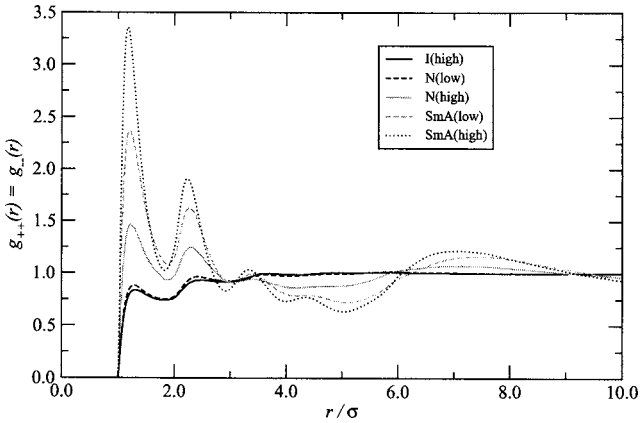

FIG. 15. The pair radial distribution function $g_{++}(r)$ for a system of 1020 charged hard spherocylinders of aspect ratio $L/\sigma=5$ at a temperature of $T^*=0.5$, obtained by Monte Carlo computer simulations and the Wolf method in the *NPT* ensemble. The lines correspond to the results for the same states shown in Fig. 14.

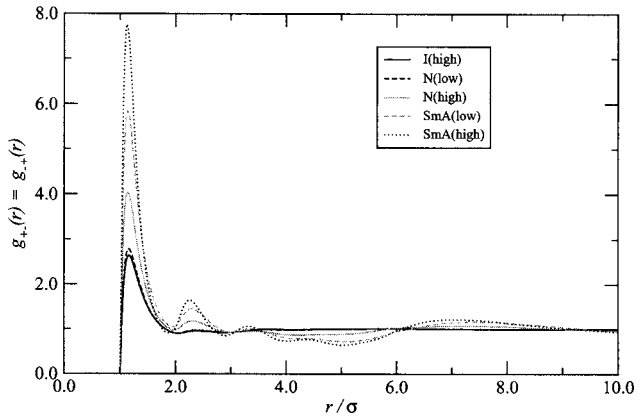

FIG. 16. The pair radial distribution function $g_{+-}(r)$ for a system of 1020 charged hard spherocylinders of aspect ratio $L/\sigma=5$ at a temperature of $T^*=0.5$, obtained by Monte Carlo computer simulations and the Wolf method in the *NPT* ensemble. The lines correspond to the results for the same states shown in Fig. 14.

particularly at lower temperatures, is required in order to determine if an *I-N*-Sm triple point occurs where the nematic phase disappears, as it happens with DHSC with longitudinal and transverse dipoles.

With respect to the smectic phases, a clear indication of ion pairing can be established from the behavior of the distribution functions of the CHSC system. This phenomenon is quite interesting, since the smectic phase behaves as a quasi-two-dimensional system within the smectic layers. A true two-dimensional (2D) electroneutral Coulomb system presents a Kosterlitz-Thouless transition[45] from a plasma to a dipolar phase. The smectic phases formed by CHSC are natural systems in order to study the way the ion pairing that induces the dipolar phase appears in quasi-2D systems and could enable us to have a deeper understanding of the mechanisms involved in the true 2D Coulombic fluid.

Finally, since the RPM of spherical electrolytes is obtained as the limit $L/\sigma=0$ of the CHSC system, it should be very interesting to study how the phase behavior and the structural and thermodynamic properties of such ionic models are related to each other, particularly at high densities where the phase diagram of the liquid-solid transition of the RPM has been characterized in a series of studies by Vega *et al.*[46–49] We will address these topics in future communications.

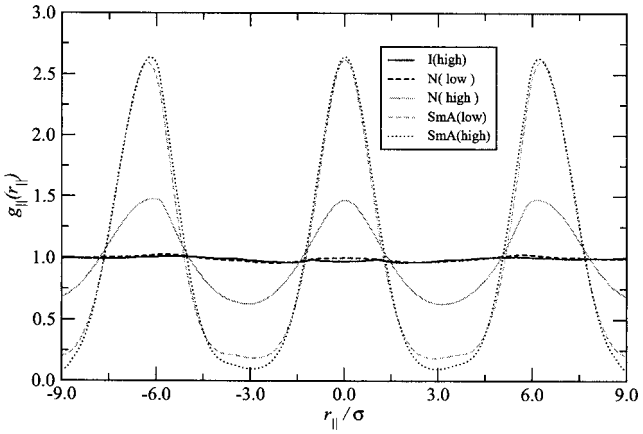

FIG. 17. The distribution function $g_{\parallel}(r_{\parallel})$ for a system of 1020 charged hard spherocylinders of aspect ratio $L/\sigma=5$ at a temperature of $T^*=0.5$, obtained by Monte Carlo computer simulations and the Wolf method in the *NPT* ensemble. The lines correspond to the results for the same states shown in Fig. 14.

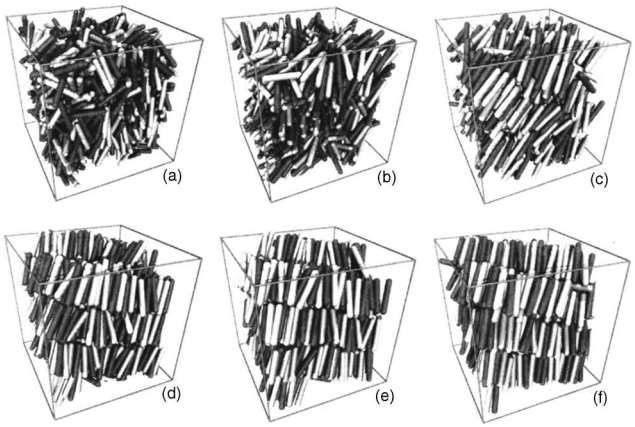

FIG. 18. Snapshots for different configurations for 1020 charged hard spherocylinders of aspect ratio $L/\sigma=5$ at a temperature of $T^*=0.5$, obtained by Monte Carlo computer simulations and the Wolf method in the *NPT* ensemble. The configurations correspond to (a) the highest-density isotropic state ($P^*=5.25$), (b) the lowest-density nematic state ($P^*=5.50$), (c) the highest-density nematic state ($P^*=6.25$), (d) the lowest-density smectic-A state ($P^*=6.50$), (e) a middle-density smectic-A state ($P^*=7.50$), and (f) the highest-density smectic-A state ($P^*=8.25$).

ACKNOWLEDGMENTS

This work was supported under CONACYT Grant No. 2007-61418. C.A. acknowledges a Ph.D. scholarship from CONACYT. They also acknowledge support from PIFI 3.3-PROMEP (México).

[1] D. van der Beek and H. N. W. Lekkerkerker, Langmuir **20**, 8582 (2004).
[2] H. Maeda and Y. Maeda, Phys. Rev. Lett. **90**, 018303 (2003).
[3] L. Onsager, Ann. N.Y. Acad. Sci. **51**, 627 (1949).
[4] S. L. Brenner and V. A. Parsegian, Biophys. J. **14**, 327 (1974).
[5] A. Stroobants, H. N. W. Lekkerkerker, and T. Odijk, Macromolecules **19**, 2232 (1986).
[6] T. Sato and A. Teramoto, Physica A **176**, 72 (1991).
[7] G. J. Vroege and H. N. W. Lekkerkerker, Rep. Prog. Phys. **55**, 1241 (1992).
[8] H. Löwen, Phys. Rev. Lett. **72**, 424 (1994).
[9] S. B. Chen and D. L. Koch, J. Chem. Phys. **104**, 359 (1996).
[10] H. Graf and H. Löwen, Phys. Rev. E **59**, 1932 (1999).
[11] H. H. Wensink, J. Chem. Phys. **126**, 194901 (2007).
[12] E. M. Kramer and J. Herzfeld, J. Chem. Phys. **110**, 8825 (1999).
[13] E. M. Kramer and J. Herzfeld, Phys. Rev. E **61**, 6872 (2000).
[14] S. C. McGrother, D. C. Williamson, and G. Jackson, J. Chem. Phys. **104**, 6755 (1996).
[15] P. Bolhuis and D. Frenkel, J. Chem. Phys. **106**, 666 (1997).
[16] M. P. Allen, G. T. Evans, D. Frenkel, and B. M. Mulder, Adv. Chem. Phys. **86**, 1 (1993).
[17] J. J. Weis, D. Levesque, and G. J. Zarragoicoechea, Phys. Rev. Lett. **69**, 913 (1992).
[18] D. Levesque, J. J. Weis, and G. J. Zarragoicoechea, Phys. Rev. E **47**, 496 (1993).
[19] J. J. Weis, D. Levesque, and G. J. Zarragoicoechea, Mol. Phys. **80**, 1077 (1993).
[20] S. C. McGrother, A. Gil-Villegas, and G. Jackson, J. Phys.: Condens. Matter **8**, 9649 (1996).
[21] A. Gil-Villegas, S. C. McGrother, and G. Jackson, Mol. Phys. **92**, 723 (1997).
[22] A. Gil-Villegas, S. C. McGrother, and G. Jackson, Chem. Phys. Lett.

269, 441 (1997).
[23] S. C. McGrother, A. Gil-Villegas, and G. Jackson, Mol. Phys. **95**, 657 (1998).
[24] A. Gil-Villegas, G. Jackson, and S. C. McGrother, J. Mol. Liq. **76**, 171 (1998).
[25] J. S. van Duijneveldt, A. Gil-Villegas, G. Jackson, and M. P. Allen, J. Chem. Phys. **112**, 9092 (2000).
[26] S. W. De Leeuw, J. W. Perram, and E. R. Smith, Proc. R. Soc. London **A373**, 26 (1980).
[27] S. W. De Leeuw, J. W. Perram, and E. R. Smith, Proc. R. Soc. London **A373**, 57 (1980).
[28] S. W. De Leeuw, J. W. Perram, and E. R. Smith, Proc. R. Soc. London, Ser. A **177**, 388 (1983).
[29] L. Onsager, J. Am. Chem. Soc. **58**, 1486 (1936).
[30] D. Wolf, Phys. Rev. Lett. **68**, 3315 (1992).
[31] D. Wolf, P. Keblinski, S. R. Phillpot, and J. Eggebrecht, J. Chem. Phys. **110**, 8254 (1999).
[32] P. Demontis, S. Spanu, and G. B. Suffritti, J. Chem. Phys. **114**, 7980 (2001).
[33] D. Zahn, B. Schilling, and S. M. Kast, J. Phys. Chem. B **106**, 10725 (2002).
[34] Y. Ma and S. H. Garofalini, Mol. Simul. **31**, 739 (2005).
[35] C. Avendaño and A. Gil-Villegas, Mol. Phys. **104**, 1475 (2006).
[36] C. Avendaño, N. Ibarra-Ávalos, C. M. Quezada, J. Medina, and A. Gil-Villegas, Rev. Mex. Fis. **S52**, 85 (2006).
[37] J. A. Moreno-Razo, E. Díaz-Herrera, and S. H. L. Klapp, Mol. Phys. **104**, 2841 (2006).
[38] C. J. Fennell and J. D. Gezelter, J. Chem. Phys. **124**, 234104 (2006).
[39] T. S. Mahadevan and S. H. Garofalini, J. Phys. Chem. B **111**, 8919 (2007).
[40] A. Carré, L. Berthier, J. Horbach, S. Ispas, and W. Kob, J. Chem. Phys. **127**, 114512 (2007).
[41] M. P. Allen and D. J. Tildesley, *Computer Simulation of Liquids* (Oxford University Press, Oxford, 1987).
[42] D. Frenkel and B. Smit, *Understanding Molecular Simulation* (Academic, London, 2002).
[43] D. Frenkel, J. Phys. Chem. **92**, 3280 (1988).
[44] A. V. Emelyanenko and M. A. Osipov, Liq. Cryst. **26**, 187 (1999).
[45] J. M. Kosterlitz and D. J. Thouless, J. Phys. C **6**, 1181 (1973).
[46] C. Vega, F. Bresme, and J. L. F. Abascal, Phys. Rev. E **54**, 2746 (1996).
[47] F. Bresme, C. Vega, and J. L. F. Abascal, Phys. Rev. Lett. **85**, 3217 (2000).
[48] J. L. F. Abascal, C. Vega, C. McBride, and F. Bresme, Phys. Rev. E **68**, 052501 (2003).
[49] C. Vega, J. L. F. Abascal, C. McBride, and F. Bresme, J. Chem. Phys. **119**, 964 (2003).